Fractional Brownian motion with fluctuating diffusivities

Adrian Pacheco-Pozo and Diego Krapf[*]

Department of Electrical and Computer Engineering and School of Biomedical Engineering,
Colorado State University, Fort Collins, Colorado 80523, USA

Despite the success of fractional Brownian motion (fBm) in modeling systems that exhibit anomalous diffusion due to temporal correlations, recent experimental and theoretical studies highlight the necessity for a more comprehensive approach of a generalization that incorporates heterogeneities in either the tracers or the environment. This work presents a modification of Lévy's representation of fBm for the case in which the generalized diffusion coefficient is a stochastic process. We derive analytical expressions for the autocovariance function and both ensemble- and time-averaged mean squared displacements. Further, we validate the efficacy of the developed framework in two-state systems, comparing analytical asymptotic expressions with numerical simulations.

I. INTRODUCTION

Anomalous diffusion processes are widespread in diverse disciplines, including nanoscale physics [1], cell and molecular biology [2–6], ecology [7,8], and finance [9–11]. These processes are characterized by a nonlinear time dependence of the mean square displacement (MSD), typically taking a power-law form $\langle X^2(t)\rangle \propto t^\alpha$ with an anomalous exponent $0 < \alpha < 2$. Here, the angular brackets denote averaging over an ensemble of trajectories. The diffusion is classified as subdiffusive when $0 < \alpha < 1$ and superdiffusive when $1 < \alpha < 2$. Normal diffusion is recovered in the limiting case $\alpha = 1$. Several mathematical models have been proposed to reproduce such MSD [12–17]. Among these models, fractional Brownian motion (fBm), a Gaussian process possessing temporal correlations [18,19], has been widely used to model systems exhibiting anomalous diffusion with temporal correlations [20–25].

Despite the success of fBm in modeling correlated random walks, experimental measurements often reveal marked heterogeneities in biological environments, highlighting the need for a generalization of fBm where its parameters change over time [26,27]. These complexities are usually due to fluctuations in the tracer particles or the medium where the diffusion takes place. Examples of such heterogeneous systems include the diffusion of proteins and lipids in the plasma membrane [28–31], intracellular transport of endosomes and lysosomes [32,33], and DNA-binding proteins [34], among others [6,35,36].

From a theoretical approach, heterogeneities have been modeled extensively as Brownian particles with fluctuating diffusivity. Examples of this type of motion include diffusing diffusivities [37,38] and the annealed transit time model [39]. To address temporal correlations in heterogeneous systems, several stochastic processes have been proposed as modifications of fBm to model heterogeneous transport [40–47]. Among them, the diffusion of particles stochastically switching between two states has been studied using numerical simulations [45]. In this previous work, each state i was characterized by a generalized diffusion coefficient D_i, a Hurst exponent H_i, and independent and identical distributed (i.i.d.) dwell times. To maintain time correlations in the switching fBm (sfBm), a modification of the integral representation of the fBm process was used [46,48]. The sfBm is of particular interest when modeling biological systems, such as the dynamics of nanoscale particles in the cytoplasm of mammalian cells [6,49]. Numerical simulations revealed asymptotic scalings of the temporal average MSD and the power spectral density. However, an analytical framework to study processes having rich dynamics, such as switching between states while keeping their temporal correlations, is still missing.

In this work, we present a framework for addressing systems exhibiting temporal correlations akin to fBm, while encompassing rich dynamics characterized by a fluctuating generalized diffusion coefficient. The presented model is valid for the diffusion coefficient being any (non-negative) stochastic process. Importantly, temporal correlations are maintained throughout the whole trajectory. The powerful yet simple applicability of the proposed framework is applied to two-state systems for which asymptotic expressions can be compared to numerical simulations. This model is closely related to the switching fBm [45] and can be seen as a generalization of the uncorrelated dichotomous model studied in Ref. [50]. We focus on dichotomous processes with dwell times that have either an exponential or a heavy-tailed distribution, which are both relevant to diffusion in complex systems. Exponential distributions of switching times have been observed for the motion of inert particles in the cytoplasm of live cells [6,49,51]. Heavy-tailed power-law distributions in the dwell times yield aging and nonergodicity, and they have been observed for protein dynamics in the plasma membrane [4,31,52], intracellular transport of insulin granules [53], and the internal dynamics in globular proteins [5,54,55].

————
[*]Contact author: diego.krapf@colostate.edu

This article is structured as follows: In Sec. II, we derive the general framework that will be used in the context of two-state systems. In Sec. III, we introduce two-state systems and, using our framework, derive the corresponding asymptotic expressions for the MSD, which we then compare with numerical simulations for each particular case. Section IV presents a summary and concluding remarks.

II. FRAMEWORK FOR $D(t)$ BEING A STOCHASTIC PROCESS

Mandelbrot's fBm $B_H(t)$ is a zero-mean, continuous Gaussian process, characterized by a Hurst exponent $H \in (0, 1)$ related to the anomalous exponent by $H = \alpha/2$ [19]. It is defined by an autocovariance,

$$\langle B_H(t_1)B_H(t_2) \rangle = D\big(t_1^{2H} + t_2^{2H} - |t_1 - t_2|^{2H}\big), \quad (1)$$

where D is the generalized diffusion coefficient with units of length^2/time^{2H}. From Eq. (1) follows that the MSD exhibits anomalous diffusion of the form

$$\langle B_H^2(t) \rangle = 2Dt^{2H}. \quad (2)$$

The motion is then classified according to the value of H as subdiffusion when $0 < H < 1/2$ and as superdiffusion when $1/2 < H < 1$. Standard Brownian motion is recovered for $H = 1/2$. An alternative form of fBm consists of Lévy's nonequilibrated formulation [48], which is written in terms of the Riemann-Liouville fractional integral as

$$B_H(t) = \sqrt{4HD} \int_0^t (t-\tau)^{H-1/2} \xi(\tau)d\tau, \quad (3)$$

where $\xi(t)$ is zero-mean Gaussian white noise with δ correlations, that is, $\langle \xi(t) \rangle = 0$, and $\langle \xi(t_1)\xi(t_2) \rangle = \delta(t_2 - t_1)$.

Following recent works [45,46], we consider fractional Brownian motion with fluctuating diffusivity as the process in Eq. (3) with a generalized diffusion coefficient being a stochastic process $D(t)$,

$$X(t) = \sqrt{4H} \int_0^t \sqrt{D(\tau)}\,(t-\tau)^{H-1/2}\,\xi(\tau)d\tau. \quad (4)$$

This process has two sources of randomness: one due to variations of the Brownian motion or Gaussian white noise $\xi(t)$, and another due to the generalized diffusion coefficient $D(t)$ being a stochastic process. Thus, when computing the mean of an observable Q, denoted as $\langle Q \rangle$, two averages must be taken: one over the Gaussian noise, denoted as $\langle \cdots \rangle_\xi$, and one over the different realizations of the generalized diffusion coefficient $D(t)$, denoted as $\langle \cdots \rangle_D$, and therefore $\langle Q \rangle = \langle \langle Q \rangle_\xi \rangle_D$. We will refer to the first average as the average over the noise, whereas the second average will be denoted as an average over the disorder.

A. Mean square displacement

To find the MSD $\langle X^2(t) \rangle$, we first average over the noise,

$$\langle X^2(t) \rangle_\xi = 4H \int_0^t dt_1 \int_0^t dt_2 \sqrt{D(t_1)D(t_2)}$$
$$\times (t-t_1)^{H-1/2}(t-t_2)^{H-1/2}\langle \xi(t_1)\xi(t_2) \rangle_\xi. \quad (5)$$

Because the white noise $\xi(t)$ is δ correlated, this expression simplifies to

$$\langle X^2(t) \rangle_\xi = 4H \int_0^t D(t_1)(t-t_1)^{2H-1}dt_1. \quad (6)$$

Next, we average over the disorder, obtaining

$$\langle \langle X^2(t) \rangle_\xi \rangle_D = 4H \int_0^t \langle D(t_1) \rangle_D\,(t-t_1)^{2H-1}dt_1, \quad (7)$$

which has the form of a convolution, with a Laplace transform that can be written as

$$\langle X^2(s) \rangle = \frac{2\,\Gamma(2H+1)}{s^{2H}}\langle D(s) \rangle_D, \quad (8)$$

where $\Gamma(x)$ is the Gamma function. Thus, by finding the Laplace transform of the mean of the generalized diffusion coefficient process $\langle D(s) \rangle$, the MSD can be readily obtained. In what follows, we will drop, for convenience, the subscript D.

When the generalized diffusion coefficient $D(t)$ is a stationary process, its mean is time independent ($\langle D_{st}(t) \rangle = \langle D_{st} \rangle$) and can be taken out of the integral in Eq. (7). So, the MSD reduces to

$$\langle X_{st}^2(t) \rangle = 2\langle D_{st} \rangle t^{2H}, \quad (9)$$

which has the well-known form of Eq. (2) with effective diffusivity $\langle D_{st} \rangle$.

B. Autocovariance

The covariance function can be expressed as

$$\langle X(t_1)X(t_2) \rangle = \tfrac{1}{2}[\langle X^2(t_1) \rangle + \langle X^2(t_2) \rangle$$
$$- \langle [X(t_2) - X(t_1)]^2 \rangle]. \quad (10)$$

The first two terms on the right-hand side of this expression are the MSD [Eq. (7)] at times t_1 and t_2. The last term corresponds to the mean of the squared increments, which can be found using a similar procedure as that of Ref. [56]. Assuming, without loss of generality, that $t_2 > t_1$, we write the increments as

$$X(t_2) - X(t_1) = \int_{t_1}^{t_2} \sqrt{4HD(u)}$$
$$\times (t_2 - u)^{H-1/2}\xi(u)du + \int_0^{t_1} \sqrt{4HD(v)}$$
$$\times [(t_2 - v)^{H-1/2} - (t_1 - v)^{H-1/2}]\xi(v)dv. \quad (11)$$

Then, taking the square of this quantity and averaging it first over the noise and then over the disorder as in Eqs. (5)–(7), we can write the mean of the squared increments as

$$\langle [X(t_2) - X(t_1)]^2 \rangle$$
$$= 4H \int_{t_1}^{t_2} \langle D(u) \rangle (t_2 - u)^{2H-1}du$$
$$+ 4H \int_0^{t_1} \langle D(v) \rangle [(t_2 - v)^{H-1/2} - (t_1 - v)^{H-1/2}]^2 dv. \quad (12)$$

Let us now introduce the variable $\tau = t_2 - t_1$ and make the change of variables $w = (t_1 - v)/\tau$, which allow us to rewrite the last equation as

$$
\langle [X(t_2) - X(t_1)]^2 \rangle
$$
$$
= 4H \int_{t_1}^{t_2} \langle D(u) \rangle (t_2 - u)^{2H-1} du + 4H\tau^{2H}
$$
$$
\times \int_0^{t_1/\tau} \langle D(t_1 - \tau w) \rangle [(1+w)^{H-1/2} - w^{H-1/2}]^2 dw. \tag{13}
$$

Next, working in the limit $t_1/\tau \to 0$, the second integral vanishes and this last expression takes the form

$$
\langle [X(t_1) - X(t_2)]^2 \rangle
$$
$$
= 4H \int_{t_1}^{t_2} \langle D(u) \rangle (t_2 - u)^{2H-1} du, \tag{14}
$$

which depends on the form of $\langle D(t) \rangle$. This limit ensures that fBm, as defined in Eq. (4), with constant generalized diffusion coefficient has the same properties as the Mandelbrot's fBm [19]. For the case where the process $D(t)$ is stationary, this last integral can be solved exactly and, for any t_1 and t_2, it reads

$$
\langle [X_{\text{st}}(t_1) - X_{\text{st}}(t_2)]^2 \rangle = 2\langle D_{\text{st}} \rangle |t_1 - t_2|^{2H}. \tag{15}
$$

Thus, the covariance function [Eq. (10)] is

$$
\langle X_{\text{st}}(t_1) X_{\text{st}}(t_2) \rangle = \langle D_{\text{st}} \rangle \big[t_1^{2H} + t_2^{2H} - |t_1 - t_2|^{2H} \big], \tag{16}
$$

which has the form of Eq. (1). From this last equation and Eq. (9), it is clear that when the process $X(t)$ has a wide-sense stationary generalized diffusion coefficient $D(t)$, it behaves as a standard fBm with an effective generalized diffusion coefficient $\langle D_{\text{st}} \rangle$.

C. Temporal average MSD

A quantity that is widely used in single-particle tracking analysis is the temporal average MSD (TAMSD), defined for an individual trajectory as

$$
\overline{\delta^2(\Delta)} = \frac{1}{T-\Delta} \int_0^{T-\Delta} [X(t+\Delta) - X(t)]^2 dt. \tag{17}
$$

Using Eq. (10), for $T \gg \Delta$, the ensemble average of the TAMSD can be written as

$$
\langle \overline{\delta^2(\Delta)} \rangle \approx \frac{1}{T} \int_0^T [\langle X^2(t+\Delta) \rangle + \langle X^2(t) \rangle
$$
$$
- 2\langle X(t+\Delta)X(t) \rangle] dt. \tag{18}
$$

Henceforth, we will refer to $\langle \overline{\delta^2(\Delta)} \rangle$ as the TAMSD. Taking the Laplace transform in the variable T on both sides,

$$
\mathcal{L}_T[T\langle \overline{\delta^2(\Delta)} \rangle] = \frac{1}{s} \mathcal{L}_t[\langle X^2(t+\Delta) \rangle + \langle X^2(t) \rangle
$$
$$
- 2\langle X(t+\Delta)X(t) \rangle], \tag{19}
$$

where we have introduced a subscript on the Laplace transforms to remove any possible ambiguity as to which variable is being used, T or t. The first term on the right-hand side of Eq. (19) corresponds to the Laplace transform of a "shifted"

MSD, whereas the second one corresponds to the Laplace transform of the MSD. This expression, then, takes the form

$$
\mathcal{L}_T[T\langle \overline{\delta^2(\Delta)} \rangle] = \frac{1}{s} \{ (e^{\Delta s} + 1)\langle X^2(s) \rangle
$$
$$
- 2\mathcal{L}_t[\langle X(t+\Delta)X(t) \rangle] \}. \tag{20}
$$

The exact Laplace transform for the covariance function involves a modified Bessel function of the second kind and is presented in Appendix A. Here, we are mostly interested in the large time asymptotics, which correspond to the small-s behavior. In this regime, the Laplace transform has the form

$$
\mathcal{L}_t[\langle X(t+\Delta)X(t) \rangle]
$$
$$
= 2\langle D(s) \rangle \frac{\Gamma(2H+1)}{s^{2H}}
$$
$$
\times \left[1 + \frac{\Delta s}{2} - \frac{\Gamma(1-H)}{\Gamma(H+1)} \left(\frac{\Delta s}{4} \right)^{2H} + O(s^{2H+1}) \right], \tag{21}
$$

where $O(s^n)$ is Landau's big-O notation. By substituting this result into Eq. (20) and taking into account that $e^{\Delta s} = 1 + \Delta s + O(s^2)$, the final expression reads

$$
\mathcal{L}_T[T\langle \overline{\delta^2(\Delta)} \rangle] = \frac{\langle D(s) \rangle}{s} \frac{\Gamma(2H+1)\Gamma(1-H)}{4^{2H-1}\Gamma(H+1)} \Delta^{2H}. \tag{22}
$$

Finally, taking the inverse Laplace transform, we obtain the TAMSD in time domain,

$$
\langle \overline{\delta^2(\Delta)} \rangle = \frac{1}{T} \mathcal{L}_T^{-1} \left[\frac{\langle D(s) \rangle}{s} \right] \frac{\Gamma(2H+1)\Gamma(1-H)}{4^{2H-1}\Gamma(H+1)} \Delta^{2H}, \tag{23}
$$

for $T \gg \Delta$. For $H = 1/2$, the result for Brownian motion with fluctuating diffusivity is recovered [50]. Moreover, when the process $D(t)$ is wide-sense stationary, one has

$$
\langle D_{\text{st}}(s) \rangle = \frac{\langle D_{\text{st}} \rangle}{s}, \tag{24}
$$

which is the Laplace transform of a constant. Then, under the wide-sense stationarity condition, Eq. (23) reduces to

$$
\langle \overline{\delta^2(\Delta)} \rangle = \frac{\Gamma(2H+1)\Gamma(1-H)}{4^{2H-1}\Gamma(H+1)} \langle D_{\text{st}} \rangle \Delta^{2H}, \tag{25}
$$

from which, by comparison with Eq. (9), one concludes that the system exhibits ultraweak ergodicity breaking, that is, the time- and ensemble-averaged MSDs have the same scaling but the prefactor is different. The prefactor in the TAMSD approaches 4 as H approaches zero (i.e., double the prefactor of the ensemble-averaged MSD) and it diverges as H approaches unity, i.e., the ballistic case. In the whole range $0 \leqslant H \leqslant 1$, this prefactor is bounded below by 2, reaching this minimum when $H = 1/2$ (standard Brownian motion). Thus, when $H = 1/2$, the ergodic behavior is recovered.

III. TWO-STATE SYSTEM WITH HEAVY-TAILED SOJOURN TIMES

To illustrate the advantages of our approach, we consider a two-state system. In this model, the particle can be in the states "+" or "−." These states are characterized by generalized diffusion coefficients, D^+ and D^-, and dwell time distributions,

$\psi_+(t)$ and $\psi_-(t)$. Both states are considered to have the same Hurst exponent H. This class of switching fBm models has been analyzed in Ref. [45] using numerical simulations and is related to the Brownian with fluctuating diffusivity studied in Ref. [50].

We consider dwell times that either have a heavy-tailed distribution with infinite mean or are exponentially distributed. Typical heavy-tailed distributions are asymptotically described by a power law of the form

$$\psi_{\text{PL}}(t) \sim \frac{a}{|\Gamma(-\alpha)|t^{1+\alpha}}, \tag{26}$$

where $0 < \alpha < 1$ and a is a constant. The condition $\alpha < 1$ leads to t not having a first moment. The Laplace transform of $\psi_{\text{PL}}(t)$, i.e., the moment generating function (MGF) of the dwell times, is

$$\psi_{\text{PL}}(s) = 1 - as^\alpha + O(s). \tag{27}$$

When $\psi_\pm$ are exponential distributions, all the moments exist and we have

$$\psi_{\text{exp}}(t) = \frac{1}{\tau}\exp\left(-t/\tau\right), \tag{28}$$

with τ being the first moment. The Laplace transform of this distribution (MGF of the dwell times) is

$$\psi_{\text{exp}}(s) = \frac{1}{1+\tau s} = 1 - \tau s + O(s^2), \tag{29}$$

where the right-hand side is useful for small-s (large-t) approximations.

When at least one of the two distributions $\psi_\pm(t)$ has a heavy-tailed form with infinite mean, the two-state system does not reach a steady state [50]. Nevertheless, regardless of the distributions being of power-law or exponential form, the first moment of the process $D(t)$ in Laplace domain has the general small-s asymptotic [50],

$$\langle D(s) \rangle \approx \frac{A}{s} + B\frac{\Gamma(\beta)}{s^\beta}, \tag{30}$$

where A, B, and β are constants that depend on $\psi_\pm(s)$. Taking the inverse Laplace transform of this last expression, one finds

$$\langle D(t) \rangle \approx A + Bt^{\beta-1}, \tag{31}$$

for large t. Thus, by computing either $\langle D(s) \rangle$ at small s or $\langle D(t) \rangle$ at large t, the constants A, B, and β are found and, in turn, the statistics of the process can be readily derived, as shown below.

The asymptotic behavior of the MSD can be found by substituting Eq. (30) into Eq. (8) and taking the inverse Laplace transform,

$$\langle X^2(t) \rangle \approx 2At^{2H} + \frac{2B\Gamma(\beta)\Gamma(2H+1)}{\Gamma(\beta+2H)}t^{\beta+2H-1}, \tag{32}$$

for large t. This expression is valid for any value $0 < H < 1$. Moreover, for normal diffusion ($H = 1/2$), Eq. (32) reduces to

$$\langle X^2(t) \rangle \approx 2At + \frac{2B}{\beta}t^\beta, \tag{33}$$

which agrees with the result obtained in Ref. [50].

To find the TAMSD, we substitute Eq. (30) into Eq. (23) and invert the Laplace transform,

$$\overline{\langle \delta^2(\Delta) \rangle} = \left(A + \frac{B}{\beta}T^{\beta-1}\right)\frac{\Gamma(2H+1)\Gamma(1-H)}{4^{2H-1}\Gamma(H+1)}\Delta^{2H}, \tag{34}$$

which is also valid for any H. Comparing the time- and ensemble-averaged MSD [Eqs. (32) and (34)] also shows that the process displays ergodicity breaking.

Examples

We now consider three cases to test the fractional Brownian motion with fluctuating diffusivity in two-state systems, namely, (1) both dwell time distributions are heavy tailed with infinite mean, (2) one of the dwell time distributions has infinite mean and the second is exponential, and (3) both distributions are exponential. We assume that $D^+ > D^- > 0$. In order to compare the analytical results with numerical simulations, for asymptotic power-law distributions, we employ a Pareto distribution,

$$\psi_{\text{PL}}(t) = \frac{\alpha t_0^\alpha}{t^{\alpha+1}} \quad \text{for } t \geqslant t_0, \tag{35}$$

which has an exact Laplace transform (MGF of the dwell times),

$$\psi_{\text{PL}}(s) = \alpha t_0^\alpha s^\alpha \Gamma(-\alpha, t_0 s), \tag{36}$$

with $\Gamma(x, y)$ being the upper incomplete Gamma function. In the limit $s \to 0$, this expression takes the form of Eq. (27) with $a = \Gamma(1-\alpha)t_0^\alpha$.

A. Case 1: Diverging mean dwell times, $0 < \alpha_\pm < 1$

For $\alpha_\pm \in (0, 1)$, with $\alpha_+ > \alpha_-$, the asymptotic behavior of the mean generalized diffusion coefficient takes the form [50]

$$\langle D(t) \rangle \approx D^- + \frac{a_+}{a_-}\frac{(D^+ - D^-)t^{\alpha_- - \alpha_+}}{\Gamma(\alpha_- - \alpha_+ + 1)}, \tag{37}$$

which converges to D^- at large times. By comparison with Eq. (31), one finds

$$A = D^-, \quad B = \frac{a_+}{a_-}\frac{(D^+ - D^-)}{\Gamma(\beta)}, \quad \text{and } \beta = \alpha_- - \alpha_+ + 1. \tag{38}$$

Therefore, the asymptotic behavior of the MSD is

$$\langle X^2(t) \rangle \approx 2D^-t^{2H}$$
$$+ 2\frac{a_+}{a_-}\frac{\Gamma(2H+1)(D^+ - D^-)}{\Gamma(\alpha_- - \alpha_+ + 2H + 1)}t^{\alpha_- - \alpha_+ + 2H}, \tag{39}$$

which converges to $2D^-t^{2H}$ at large t.

In order to evaluate this type of two-state systems, we simulated 1000 trajectories of fractional Brownian motion with fluctuating diffusivity (see Appendix B) with $H = 0.3$, $D^+ = 10$, $D^- = 1$, $\alpha_+ = 0.75$, $\alpha_- = 0.25$, $t_{0,+} = 3$, and $t_{0,-} = 25$. All the realizations start in the "+" state. Figure 1(a) shows one trajectory $X(t)$ alongside the process $D(t)$ used to compute it. Figure 1(b) shows the analytical MSD together with the numerical simulation results. The asymptotic behavior given by Eq. (39) presents a crossover between two regimes
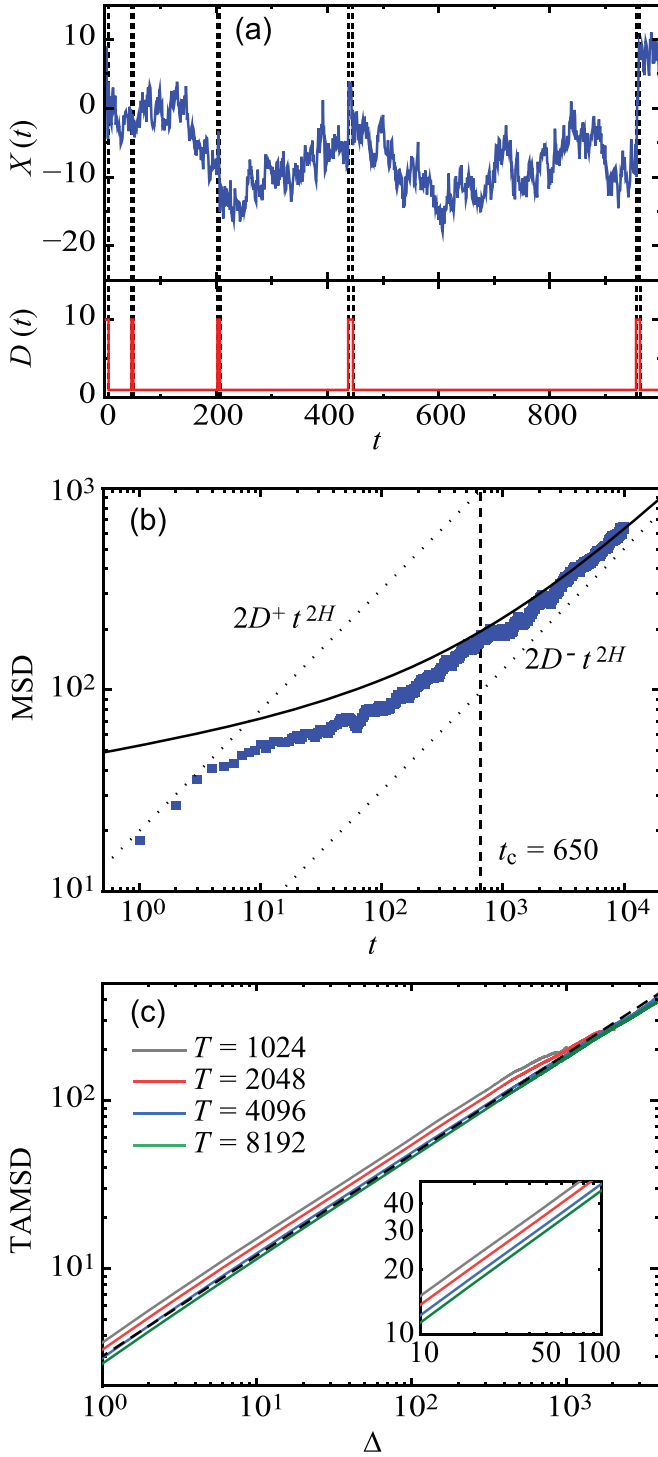
FIG. 1. Case 1: Two-state system where both states have heavy-tailed dwell time distributions. The parameters in this example are $D^+ = 10$, $D^- = 1$, $\alpha_+ = 0.75$, $\alpha_- = 0.25$, $t_{0,+} = 3$, and $t_{0,-} = 25$. (a) Representative trajectory $X(t)$ together with $D(t)$. (b) The MSD is shown for numerical simulations as blue squares. The solid line shows the analytical asymptotic behavior given by Eq. (39) and the dotted lines show the MSD of each of the two states. (c) TAMSD for different realization times; the dashed line represents the analytical asymptotic behavior given by Eq. (41) for $T = 8192$. Inset: A close-up to highlight the dependence of TAMSD on the realization time T.

with $\langle X^2(t) \rangle \sim t^{2H}$ and $\langle X^2(t) \rangle \sim t^{\alpha_+ - \alpha_- + 2H}$. This crossover takes place at the critical time

$$t_{\mathrm{c}} = \left[\frac{a_+}{a_-} \frac{\Gamma(2H+1)}{\Gamma(\alpha_- - \alpha_+ + 2H + 1)} \frac{D^+ - D^-}{D^-} \right]^{\frac{1}{\alpha_+ - \alpha_-}}, \quad (40)$$

which, here, is $t_{\mathrm{c}} = 650$. The MSD of the numerical simulations shown in Fig. 1(b) exhibits three different regimes: an initial regime where the MSD depends on the initial condition, i.e., the starting state, an intermediate regime up to a time of the order of t_c where the MSD has an anomalous exponent smaller than $2H$, and a long time asymptotic with the anomalous exponent being $2H$.

The TAMSD [Fig. 1(c)] for this case is

$$\overline{\langle \delta^2(\Delta) \rangle} = \left[D^- + \frac{a_+}{a_-} \frac{(D^+ - D^-)}{\Gamma(\alpha_- - \alpha_+ + 2)} T^{\alpha_- - \alpha_+} \right]$$
$$\times \frac{\Gamma(2H+1)\Gamma(1-H)}{4^{2H-1}\Gamma(H+1)} \Delta^{2H}. \quad (41)$$

The TAMSD exhibits a dependence on the experimental time via a scaling $T^{\alpha_- - \alpha_+}$. In the long time limit, it converges to $\Gamma(2H+1)\Gamma(1-H)/[4^{2H-1}\Gamma(H+1)]D^- \Delta^{2H}$. The large-$t$ asymptotic of the TAMSD, thus, differs from the ensemble-averaged MSD ($2D^- \Delta^{2H}$) by a constant factor, showing ultraweak ergodicity breaking.

B. Case 2: Exponential distribution $\psi_+(t)$ and heavy-tailed ψ_-, $0 < \alpha_- < 1$

For $\psi_+(t)$ being exponential and $\psi_-(t)$ being heavy tailed with $\alpha_- \in (0, 1)$, the asymptotic behavior of the mean generalized diffusion coefficient reads

$$\langle D(t) \rangle \approx D^- + \frac{\tau_+}{a_-} \frac{(D^+ - D^-)}{\Gamma(\alpha_-)} t^{\alpha_- - 1}. \quad (42)$$

A comparison with Eq. (31) shows

$$A = D^-, \quad B = \frac{\tau_+}{a_-} \frac{(D^+ - D^-)}{a_+ \Gamma(\alpha_-)}, \quad \text{and } \beta = \alpha_-. \quad (43)$$

Thus, the asymptotic behavior of the MSD is

$$\langle X^2(t) \rangle \approx 2D^- t^{2H}$$
$$+ 2\frac{\tau_+}{a_-} \frac{\Gamma(2H+1)(D^+ - D^-)}{\Gamma(\alpha_- + 2H)} t^{\alpha_- + 2H - 1}, \quad (44)$$

which converges to $2D^- t^{2H}$ at long times.

We generated 1000 realizations of the process starting in the "+" state, with $H = 0.3$, $D^+ = 10$, $D^- = 1$, $\alpha_- = 0.5$, $\tau_+ = 15$, and $t_{0,-} = 25$. Figure 2(a) shows a trajectory $X(t)$ alongside the process $D(t)$. Figure 2(b) shows a comparison between the asymptotic MSD and the one obtained from numerical simulations. In a similar way as for case 1, there is a crossover between diffusion regimes, with a crossover time

$$t_{\mathrm{c}} = \left[\frac{\tau_+}{a_-} \frac{\Gamma(2H+1)}{\Gamma(\alpha_- + 2H)} \frac{D^+ - D^-}{D^-} \right]^{1/(1-\alpha_+)}, \quad (45)$$
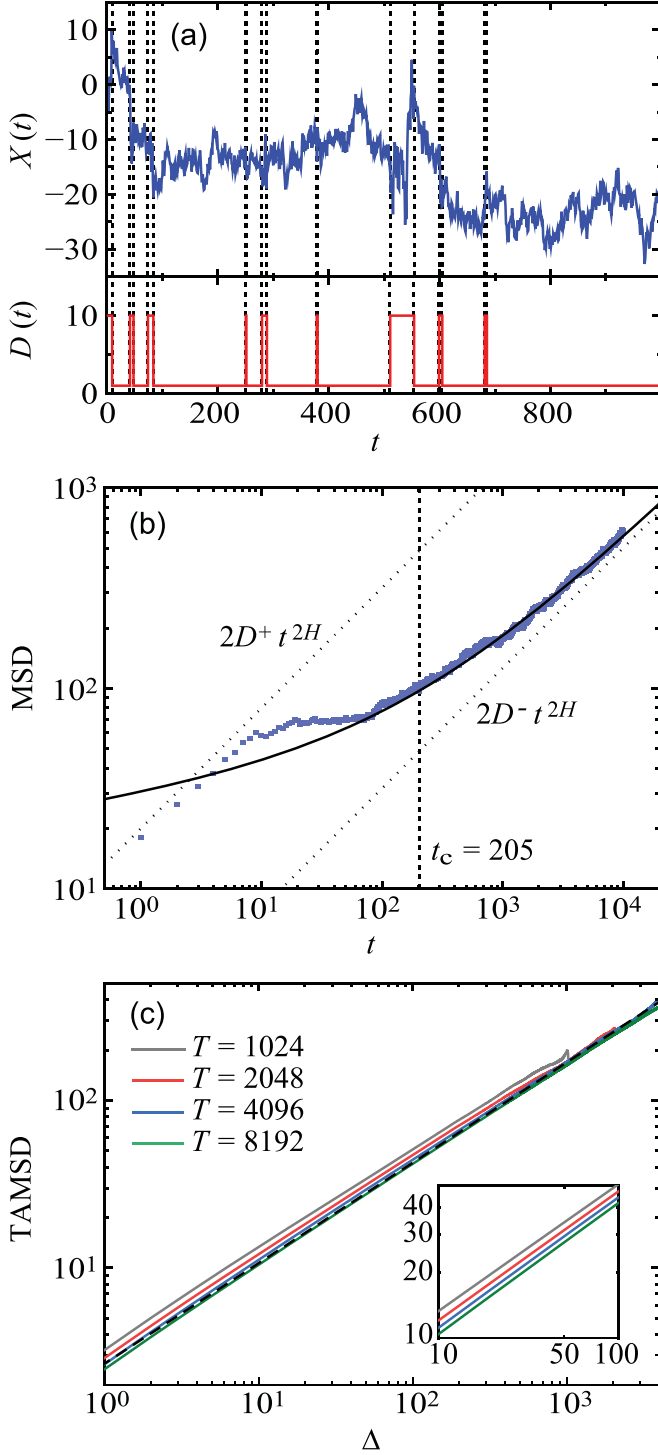
which, here, is $t_{\mathrm{c}} = 205$.

FIG. 2. Case 2: Two-state system where one state has an exponential distribution and the other state has a heavy-tailed dwell time distribution. The parameters in this example are $D^+ = 10$, $D^- = 1$, $\tau_+ = 15$, $\alpha_- = 0.5$, and $t_{0,-} = 25$. (a) Representative trajectory $X(t)$ together with $D(t)$. (b) The MSD is shown for numerical simulations as blue squares. The solid line shows the analytical asymptotic behavior given by Eq. (39) and the dotted lines show the MSD of each of the two states. (c) TAMSD for different realization times; the dashed line represents the analytical asymptotic behavior given by Eq. (41) for $T = 8192$. Inset: A close-up to highlight the dependence of TAMSD on the realization time.

The TAMSD [shown in Fig. 2(c)] is

$$\langle \overline{\delta^2(\Delta)} \rangle = \left[D^- + \frac{\tau_+}{a_-} \frac{(D^+ - D^-)}{\Gamma(\alpha_- + 1)} T^{\alpha_- - 1} \right]$$
$$\times \frac{\Gamma(2H + 1)\Gamma(1 - H)}{4^{2H-1}\Gamma(H + 1)} \Delta^{2H}, \qquad (46)$$

which, again, in the long time limit, differs from the ensemble-averaged MSD ($2D^- \Delta^{2H}$) by a constant factor (ultraweak nonergodicity).

C. Case 3: Two exponential distributions

For the case where both $\psi_\pm(t)$ are exponential, the process $D(t)$ is Markovian and its first moment converges at long times to

$$\langle D(t) \rangle = \langle D_{\text{st}} \rangle = D^+ p_{\text{eq}}^+ + D^- p_{\text{eq}}^-, \qquad (47)$$

where $p_{\text{eq}}^\pm$ is the probability that a particle is found in state $\pm$,

$$p_{\text{eq}}^\pm = \frac{\tau_\pm}{\tau_+ + \tau_-}. \qquad (48)$$

Thus, following Eq. (9), the MSD is

$$\langle X^2(t) \rangle = 2\langle D_{\text{st}} \rangle t^{2H}. \qquad (49)$$

On the other hand, the TAMSD [Eq. (25), Fig. 3(c)] is

$$\overline{\langle \delta^2(\Delta) \rangle} = \frac{\Gamma(2H + 1)\Gamma(1 - H)}{4^{2H-1}\Gamma(H + 1)} \langle D_{\text{st}} \rangle \Delta^{2H}. \qquad (50)$$

While we have not used Eq. (30) in this last example, it is possible to proceed in the same fashion as done for the previous two examples with $A = \langle D_{\text{st}} \rangle$ and $B = 0$.

A total of 1000 trajectories were simulated, all starting in the "+" state, with $H = 0.3$, $D^+ = 10$, $D^- = 1$, $\tau_+ = 15$, and $\tau_- = 25$. Figure 3(a) shows a trajectory $X(t)$ alongside the process $D(t)$. Figure 3(b) shows a comparison between the analytical MSD and the one obtained by numerical simulations. In Fig. 3(c), the TAMSD is shown for different realization times, showing that when $D(t)$ is stationary, there is no dependence on the realization time.

IV. DISCUSSION

In this work, we have studied fractional Brownian motion with fluctuating diffusivity $X(t)$, a process defined in Eq. (4) as a modification of Lévy's integral representation of the fBm for the case where the generalized diffusion coefficient is a stochastic process, $D(t)$. This process, therefore, keeps the temporal correlation, while adding an extra layer of complexity encapsulated in the stochastic dynamic of the diffusion coefficient. We derived exact expressions for the MSD [Eq. (8)] and TAMSD [Eq. (22)] in the Laplace domain. For the case when $H = 1/2$, the process in Eq. (4) reduces to a modified Brownian motion with a stochastic diffusion coefficient, for which our expressions reduce to those previously derived for such process. Additionally, when $D(t)$ is a stationary process, its first moment is constant in time, i.e., $\langle D(t) \rangle_{\text{st}} = \langle D \rangle$, and the MSD reduces to that of standard fBm with an effective diffusivity. However, because we employ Lévy's nonequilibrated representation of the fBm, this system is ultraweakly nonergodic, where the ensemble-averaged MSD has a different prefactor than that of the TAMSD.
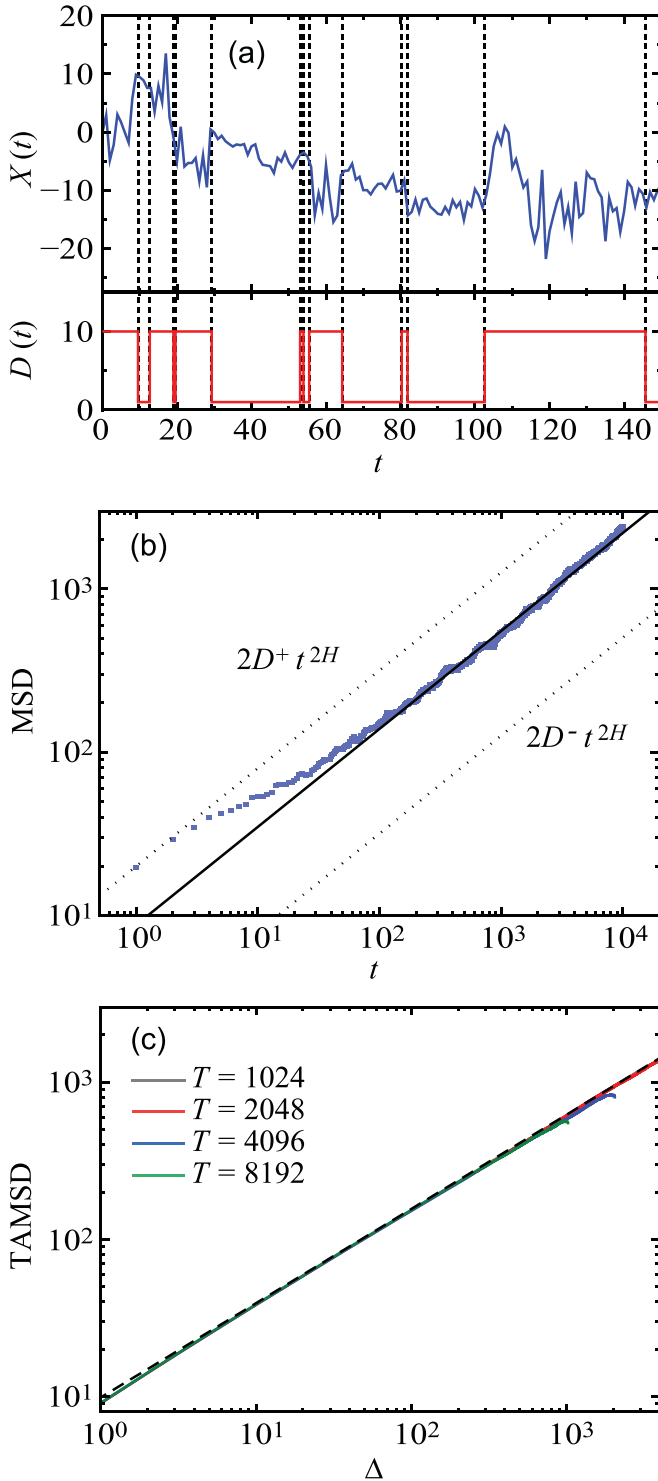
FIG. 3. Case 3: Two-state system where both states have exponential dwell time distributions. The parameters in this example are $D^+ = 10$, $D^- = 1$, $\tau_+ = 15$, and $\tau_- = 25$. (a) Representative trajectory $X(t)$ together with $D(t)$. (b) The MSD is shown for numerical simulations as blue squares. The solid line shows the analytical asymptotic behavior given by Eq. (39) and the dotted lines show the MSD of each of the two states. (c) TAMSD for different realization times; the dashed line represents the analytical asymptotic behavior given by Eq. (41) for $T = 8192$.

To test the capability of our framework, we have considered two-state processes where the diffusion coefficient follows a dichotomous stochastic process. This case is particularly relevant in modeling diffusion in the cytoplasm of live cells [6,49]. In particular, the sojourn times following an exponential distribution for one state and a power-law distribution for the other state have been observed in diverse complex systems [30,57–59]. We considered the nonequilibrium dichotomous stochastic process for which the sojourn times for one or both states can have a heavy-tailed distribution. We derived analytical expressions for these processes and found excellent agreement with the numerical simulations. With our framework, we also find analytical expressions that agree with published numerical simulations [45].

All presented numerical simulations start in a defined state. Namely, at $t = 0$, the process is in the "+" state and, thus, the MSD at small times has the behavior of that specific state [Figs. 1(b), 2(b), and 3(b)], $\langle X^2(t) \rangle = 2D^+ t^{2H}$. Nevertheless, this dependence is not seen in the TAMSD because this quantity is obtained by averaging over long times, at which the dependence on the initial condition is already lost [Figs. 1(c), 2(c), and 3(c)]. For systems that can reach equilibrium, such as the Markovian switching described in case 3, it is possible to randomize the initial state so that the system is already equilibrated at $t = 0$. Under these conditions, the dependence on the initial condition in the MSD would be eliminated. This type of randomization is highly relevant to experiments where the diffusion process initiated a long time before the measurements [6]. Given that the first two cases, when at least one of the states has a heavy-tailed dwell time distribution, do not equilibrate, randomizing the starting state does not eliminate the dependence on the initial conditions.

We have considered two-state systems with heavy-tailed dwell time distributions that asymptotically converge toward the state with smaller diffusivity. Namely, the "−" state has a smaller α exponent than the "+" state, or the latter has an exponential distribution. These conditions lead to the emergence of a crossover between two different temporal diffusion regimes in the MSD [Eqs. (39) and (44), and Figs. 1(b) and 2(b)]. In a similar fashion as that observed for Brownian motion with fluctuating diffusivities [50], if the state with the smaller α exponent has higher D, such crossover is not observed and the overall behavior involves a reduction in the MSD at small times, followed by a convergence to $2D^+ t^{2H}$.

This work opens the way for other possible generalizations, for instance, a situation in which not only the diffusion coefficient is stochastic, but also the Hurst exponent. Additionally, the two-state system, presented here as an example, could be generalized to a multistate system or even to a more complex situation where one of the states involves confinement or transient immobilization.

APPENDIX A: LAPLACE TRANSFORM OF THE COVARIANCE FUNCTION

The covariance function can be written as

$$
\langle X(t + \Delta)X(t)\rangle = 4H \int_0^t \langle D(t')\rangle
$$
$$
\times (t + \Delta - t')^{H-1/2}(t - t')^{H-1/2}dt',
$$
$$(A1)$$

which, by making the change of variable $u = t - t'$, takes the form of a convolution,

$$
\langle X(t + \Delta)X(t)\rangle = 4H\Delta^{2H-1} \int_0^t \langle D(t - u)\rangle
$$
$$
\times \left(1 + \frac{u}{\Delta}\right)^{H-1/2}\left(\frac{u}{\Delta}\right)^{H-1/2} du. \quad (A2)
$$

The Laplace transform of a convolution is known and reads

$$
\mathcal{L}(\langle X(t + \Delta)X(t)\rangle)
$$
$$
= 4H\Delta^{2H-1}\langle D(s)\rangle
$$
$$
\times \int_0^\infty e^{-us}\left(1 + \frac{u}{\Delta}\right)^{H-1/2}\left(\frac{u}{\Delta}\right)^{H-1/2} du. \quad (A3)
$$

Let us denote the integral in this expression as

$$
f(s, \Delta) = \int_0^\infty e^{-us}\left(1 - \frac{u}{\Delta}\right)^{H-1/2}\left(\frac{u}{\Delta}\right)^{H-1/2} du. \quad (A4)
$$

Then, by making the change of variable $t = us$, it can be rewritten as

$$
f(s, \Delta) = \frac{\Gamma(H + 1/2)e^{\Delta s/2}}{\pi^{1/2}\Delta^{H-1}s^H}K_H\left(\frac{\Delta s}{2}\right), \quad (A5)
$$

where $K_\nu(z)$ is the modified Bessel function of the second kind of order ν having the following integral representation [60]:

$$
K_\nu(z) = \sqrt{\frac{\pi}{2z}}\frac{e^{-z}}{\Gamma(\nu + 1/2)}
$$
$$
\times \int_0^\infty e^{-t}\left(1 - \frac{t}{2z}\right)^{\nu-1/2}t^{\nu-1/2}dt, \quad (A6)
$$

which can be expressed in terms of the modified Bessel function of the first kind $I_\nu(z)$ in the following way [60]:

$$
K_\nu(z) = \frac{\pi}{2}\frac{I_{-\nu}(z) - I_\nu(z)}{\sin(\nu\pi)}. \quad (A7)
$$

This last expression will allow us to find the asymptotic expansion for $s \to 0$. Now, the modified Bessel function of the first kind has the following series expansion [60]:

$$
I_\nu(z) = \sum_{s=0}^\infty \frac{1}{s!\Gamma(s + \nu + 1)}\left(\frac{z}{2}\right)^{2s+\nu}, \quad (A8)
$$

and, thus, the modified Bessel function of the second kind can be approximated for small s via

$$
K_H\left(\frac{\Delta s}{2}\right) = \frac{4^H\pi}{2\sin(H\pi)(\Delta s)^H\Gamma(1 - H)}
$$
$$
\times \left[1 - \frac{\Gamma(1 - H)}{\Gamma(H + 1)}\left(\frac{\Delta s}{4}\right)^{2H} + O(s^2)\right]. \quad (A9)
$$

On the other hand, the exponential function in Eq. (A5) can be expanded for $s \to 0$ as

$$
\exp\left(\frac{\Delta s}{2}\right) = 1 + \frac{\Delta s}{2} + O(s^2). \quad (A10)
$$

Then, Eq. (A5) can be rewritten as

$$
f(s, \Delta) = \frac{\Gamma(2H)}{\Delta^{2H-1}s^{2H}}\left[1 + \frac{\Delta s}{2}\right.
$$
$$
\left. - \frac{\Gamma(1 - H)}{\Gamma(H + 1)}\left(\frac{\Delta s}{4}\right)^{2H} + O(s^{2H+1})\right], \quad (A11)
$$

where we have used the following two properties of the Γ function [60]:

$$
\Gamma(x)\Gamma(1 - x) = \frac{\pi}{\sin(\pi x)} \quad (A12)
$$

and

$$
\Gamma(x + 1/2)\Gamma(x) = 2^{1-2x}\pi^{1/2}\Gamma(2x). \quad (A13)
$$

Finally, let us replace Eq. (A11) in Eq. (A3) to find the Laplace transform of the covariance function for $s \to 0$,

$$
\mathcal{L}[\langle X(t + \Delta)X(t)\rangle]
$$
$$
= 4H\langle D(s)\rangle\frac{\Gamma(2H)}{s^{2H}}
$$
$$
\times \left[1 + \frac{\Delta s}{2} - \frac{\Gamma(1 - H)}{\Gamma(H + 1)}\left(\frac{\Delta s}{4}\right)^{2H} + O(s^{2H+1})\right].
$$
$$(A14)$$

APPENDIX B: NUMERICAL METHODS

The numerical methods used to simulate fractional Brownian motion with fluctuating diffusivity closely follow the method presented in Ref. [45]. Let us start by rewriting the process under consideration, namely,

$$
X(t) = \int_0^t \sqrt{4HD(\tau)}\,(t - \tau)^{H-1/2}\,dB(\tau). \quad (B1)
$$

Further, we consider the process to start at $t = 0$ and $X(0) = 0$ and to have a realization time T. Briefly, the interval $[0, T]$ is divided in M times, $t_i = i\Delta t$, with $i = 1, 2, \ldots, M$, and $\Delta t = T/M$. From Eq. (B1), we known that the process $X(t)$ at each one of the $t = t_i$ is given by

$$
X(t_i) = \int_0^{t_i} \sqrt{4HD(\tau)}\,(t_i - \tau)^{H-1/2}\,dB(\tau). \quad (B2)
$$

Next, we divide the interval $[0, t_i]$ into N evenly spaced subintervals $[\tau_j, \tau_{j+1})$ with $j = 0, \ldots, N - 1$, $\tau_0 = 0$, $\tau_N = t_i$. The above integral can be rewritten as

$$
X(t_i) \approx \sum_{j=0}^{N-1} \int_{\tau_j}^{\tau_{j+1}} \sqrt{4HD(\tau)}\,(t_i - \tau)^{H-1/2}\,dB(\tau). \quad (B3)
$$

Each integral can then be Riemann approximated to obtain

$$
X(t_i) \approx \sum_{j=0}^{N-1} \sqrt{4HD(\tau_i)}\,(t_i - \tau_j)^{H-1/2}\,\xi_j, \quad (B4)
$$

where $\xi_j = B(\tau_{j+i}) - B(\tau_j)$ are i.i.d. Gaussian random numbers with zero mean and variance $\Delta\tau = \tau_{j+1} - \tau_j$. The simulations presented in this work have the following parameters: $\Delta t = 1$ is fixed, $M = T = 10^4$, and $\Delta\tau = 1/50$. Other parameters that were used in the simulations are found in the main text.

[1] F. Kindermann, A. Dechant, M. Hohmann, T. Lausch, D. Mayer, F. Schmidt, E. Lutz, and A. Widera, Nonergodic diffusion of single atoms in a periodic potential, Nat. Phys. **13**, 137 (2017).

[2] A. V. Weigel, B. Simon, M. M. Tamkun, and D. Krapf, Ergodic and nonergodic processes coexist in the plasma membrane as observed by single-molecule tracking, Proc. Natl. Acad. Sci. USA **108**, 6438 (2011).

[3] E. Barkai, Y. Garini, and R. Metzler, Strange kinetics of single molecules in living cells, Phys. Today **65**(8), 29 (2012).

[4] C. Manzo, J. A. Torreno-Pina, P. Massignan, G. J. Lapeyre Jr, M. Lewenstein, and M. F. Garcia Parajo, Weak ergodicity breaking of receptor motion in living cells stemming from random diffusivity, Phys. Rev. X **5**, 011021 (2015).

[5] D. Krapf and R. Metzler, Strange interfacial molecular dynamics, Phys. Today **72**(9), 48 (2019).

[6] A. Sabri, X. Xu, D. Krapf, and M. Weiss, Elucidating the origin of heterogeneous anomalous diffusion in the cytoplasm of mammalian cells, Phys. Rev. Lett. **125**, 058101 (2020).

[7] O. Vilk, E. Aghion, T. Avgar, C. Beta, O. Nagel, A. Sabri, R. Sarfati, D. K. Schwartz, M. Weiss, D. Krapf *et al.*, Unravelling the origins of anomalous diffusion: From molecules to migrating storks, Phys. Rev. Res. **4**, 033055 (2022).

[8] O. Vilk, Y. Orchan, M. Charter, N. Ganot, S. Toledo, R. Nathan, and M. Assaf, Ergodicity breaking in area-restricted search of avian predators, Phys. Rev. X **12**, 031005 (2022).

[9] J.-P. Bouchaud, The subtle nature of financial random walks, Chaos: Interdisc. J. Nonlin. Sci. **15**, 026104 (2005).

[10] E. Scalas, The application of continuous-time random walks in finance and economics, Physica A **362**, 225 (2006).

[11] V. Plerou, P. Gopikrishnan, L. A. Nunes Amaral, X. Gabaix, and H. E. Stanley, Economic fluctuations and anomalous diffusion, Phys. Rev. E **62**, R3023(R) (2000).

[12] F. Höfling and T. Franosch, Anomalous transport in the crowded world of biological cells, Rep. Prog. Phys. **76**, 046602 (2013).

[13] R. Metzler, J.-H. Jeon, A. G. Cherstvy, and E. Barkai, Anomalous diffusion models and their properties: Nonstationarity, nonergodicity, and ageing at the centenary of single particle tracking, Phys. Chem. Chem. Phys. **16**, 24128 (2014).

[14] C. Manzo and M. F. Garcia-Parajo, A review of progress in single particle tracking: From methods to biophysical insights, Rep. Prog. Phys. **78**, 124601 (2015).

[15] D. Krapf, Mechanisms underlying anomalous diffusion in the plasma membrane, Curr. Top. Membranes **75**, 167 (2015).

[16] H. Shen, L. J. Tauzin, R. Baiyasi, W. Wang, N. Moringo, B. Shuang, and C. F. Landes, Single particle tracking: From theory to biophysical applications, Chem. Rev. **117**, 7331 (2017).

[17] G. Muñoz-Gil, G. Volpe, M. A. Garcia-March, E. Aghion, A. Argun, C. B. Hong, T. Bland, S. Bo, J. A. Conejero, N. Firbas *et al.*, Objective comparison of methods to decode anomalous diffusion, Nat. Commun. **12**, 6253 (2021).

[18] A. N. Kolmogorov, Wiener spirals and some other interesting curves in a Hilbert space, in *Selected Works of A.*

N. Kolmogorov. Vol. I. Mathematics and Mechanics, edited by V. M. Tikhomirov (Kluwer Academic, Dordrecht, 1940), pp. 303–307.

[19] B. B. Mandelbrot and J. W. Van Ness, Fractional Brownian motions, fractional noises and applications, SIAM Rev. **10**, 422 (1968).

[20] J. Szymanski and M. Weiss, Elucidating the origin of anomalous diffusion in crowded fluids, Phys. Rev. Lett. **103**, 038102 (2009).

[21] G. Guigas, C. Kalla, and M. Weiss, Probing the nanoscale viscoelasticity of intracellular fluids in living cells, Biophys. J. **93**, 316 (2007).

[22] M. Magdziarz, A. Weron, K. Burnecki, and J. Klafter, Fractional Brownian motion versus the continuous-time random walk: A simple test for subdiffusive dynamics, Phys. Rev. Lett. **103**, 180602 (2009).

[23] J.-H. Jeon, V. Tejedor, S. Burov, E. Barkai, C. Selhuber-Unkel, K. Berg-Sørensen, L. Oddershede, and R. Metzler, In vivo anomalous diffusion and weak ergodicity breaking of lipid granules, Phys. Rev. Lett. **106**, 048103 (2011).

[24] J.-H. Jeon, N. Leijnse, L. B. Oddershede, and R. Metzler, Anomalous diffusion and power-law relaxation of the time averaged mean squared displacement in wormlike micellar solutions, New J. Phys. **15**, 045011 (2013).

[25] S. Sadegh, J. L. Higgins, P. C. Mannion, M. M. Tamkun, and D. Krapf, Plasma membrane is compartmentalized by a self-similar cortical actin meshwork, Phys. Rev. X **7**, 011031 (2017).

[26] T. A. Waigh and N. Korabel, Heterogeneous anomalous transport in cellular and molecular biology, Rep. Prog. Phys. **86**, 126601 (2023).

[27] Y. Lanoiselée, N. Moutal, and D. S. Grebenkov, Diffusion-limited reactions in dynamic heterogeneous media, Nat. Commun. **9**, 4398 (2018).

[28] W. He, H. Song, Y. Su, L. Geng, B. J. Ackerson, H. Peng, and P. Tong, Dynamic heterogeneity and non-Gaussian statistics for acetylcholine receptors on live cell membrane, Nat. Commun. **7**, 11701 (2016).

[29] J.-H. Jeon, M. Javanainen, H. Martinez-Seara, R. Metzler, and I. Vattulainen, Protein crowding in lipid bilayers gives rise to non-Gaussian anomalous lateral diffusion of phospholipids and proteins, Phys. Rev. X **6**, 021006 (2016).

[30] G. Sikora, A. Wyłomańska, J. Gajda, L. Solé, E. J. Akin, M. M. Tamkun, and D. Krapf, Elucidating distinct ion channel populations on the surface of hippocampal neurons via single-particle tracking recurrence analysis, Phys. Rev. E **96**, 062404 (2017).

[31] A. Weron, K. Burnecki, E. J. Akin, L. Solé, M. Balcerek, M. M. Tamkun, and D. Krapf, Ergodicity breaking on the neuronal surface emerges from random switching between diffusive states, Sci. Rep. **7**, 5404 (2017).

[32] D. Han, N. Korabel, R. Chen, M. Johnston, A. Gavrilova, V. J. Allan, S. Fedotov, and T. A. Waigh, Deciphering anomalous heterogeneous intracellular transport with neural networks, eLife **9**, e52224 (2020).

[33] S. Fedotov and D. Han, Population heterogeneity in the fractional master equation, ensemble self-reinforcement, and strong memory effects, Phys. Rev. E **107**, 034115 (2023).

[34] C. Loverdo, O. Bénichou, R. Voituriez, A. Biebricher, I. Bonnet, and P. Desbiolles, Quantifying hopping and jumping in facilitated diffusion of DNA-binding proteins, Phys. Rev. Lett. **102**, 188101 (2009).

[35] G. Muñoz, H. Bachimanchi, J. Pineda, B. Midtvedt, M. Lewenstein, R. Metzler, D. Krapf, G. Volpe, and C. Manzo, Quantitative evaluation of methods to analyze motion changes in single-particle experiments, arXiv:2311.18100.

[36] I. Bronstein, Y. Israel, E. Kepten, S. Mai, Y. Shav-Tal, E. Barkai, and Y. Garini, Transient anomalous diffusion of telomeres in the nucleus of mammalian cells, Phys. Rev. Lett. **103**, 018102 (2009).

[37] M. V. Chubynsky and G. W. Slater, Diffusing diffusivity: A model for anomalous, yet Brownian, diffusion, Phys. Rev. Lett. **113**, 098302 (2014).

[38] A. V. Chechkin, F. Seno, R. Metzler, and I. M. Sokolov, Brownian yet non-Gaussian diffusion: From superstatistics to subordination of diffusing diffusivities, Phys. Rev. X **7**, 021002 (2017).

[39] P. Massignan, C. Manzo, J. A. Torreno-Pina, M. F. García-Parajo, M. Lewenstein, and G. J. Lapeyre Jr, Nonergodic subdiffusion from Brownian motion in an inhomogeneous medium, Phys. Rev. Lett. **112**, 150603 (2014).

[40] W. Wang, F. Seno, I. M. Sokolov, A. V. Chechkin, and R. Metzler, Unexpected crossovers in correlated random-diffusivity processes, New J. Phys. **22**, 083041 (2020).

[41] W. Wang, A. G. Cherstvy, A. V. Chechkin, S. Thapa, F. Seno, X. Liu, and R. Metzler, Fractional Brownian motion with random diffusivity: Emerging residual nonergodicity below the correlation time, J. Phys. A: Math. Theor. **53**, 474001 (2020).

[42] Z. R. Fox, E. Barkai, and D. Krapf, Aging power spectrum of membrane protein transport and other subordinated random walks, Nat. Commun. **12**, 6162 (2021).

[43] D. Szarek, I. Jabłoński, D. Krapf, and A. Wyłomańska, Multifractional Brownian motion characterization based on Hurst exponent estimation and statistical learning, Chaos: Interdisc. J. Nonlin. Sci. **32**, 083148 (2022).

[44] M. Balcerek, K. Burnecki, S. Thapa, A. Wyłomańska, and A. Chechkin, Fractional Brownian motion with random Hurst exponent: Accelerating diffusion and persistence transitions, Chaos: Interdisc. J. Nonlin. Sci. **32**, 093114 (2022).

[45] M. Balcerek, A. Wyłomańska, K. Burnecki, R. Metzler, and D. Krapf, Modelling intermittent anomalous diffusion with switching fractional Brownian motion, New J. Phys. **25**, 103031 (2023).

[46] W. Wang, M. Balcerek, K. Burnecki, A. V. Chechkin, S. Janušonis, J. Ślezak, T. Vojta, A. Wyłomańska, and R. Metzler, Memory-multi-fractional Brownian motion with continuous correlations, Phys. Rev. Res. **5**, L032025 (2023).

[47] J. Ślezak and R. Metzler, Minimal model of diffusion with time changing Hurst exponent, J. Phys. A: Math. Theor. **56**, 35LT01 (2023).

[48] P. Lévy, *Random Functions: General Theory with Special Reference to Laplacian Random Functions*, University of California Publications in Statistics (University of California Press, Berkeley, California, 1953).

[49] J. Janczura, M. Balcerek, K. Burnecki, A. Sabri, M. Weiss, and D. Krapf, Identifying heterogeneous diffusion states in the cytoplasm by a hidden Markov model, New J. Phys. **23**, 053018 (2021).

[50] T. Miyaguchi, T. Akimoto, and E. Yamamoto, Langevin equation with fluctuating diffusivity: A two-state model, Phys. Rev. E **94**, 012109 (2016).

[51] C. Dieball, D. Krapf, M. Weiss, and A. Godec, Scattering fingerprints of two-state dynamics, New J. Phys. **24**, 023004 (2022).

[52] A. V. Weigel, M. M. Tamkun, and D. Krapf, Quantifying the dynamic interactions between a clathrin-coated pit and cargo molecules, Proc. Natl. Acad. Sci. USA **110**, E4591 (2013).

[53] S. A. Tabei, S. Burov, H. Y. Kim, A. Kuznetsov, T. Huynh, J. Jureller, L. H. Philipson, A. R. Dinner, and N. F. Scherer, Intracellular transport of insulin granules is a subordinated random walk, Proc. Natl. Acad. Sci. USA **110**, 4911 (2013).

[54] X. Hu, L. Hong, M. Dean Smith, T. Neusius, X. Cheng, and J. C. Smith, The dynamics of single protein molecules is nonequilibrium and self-similar over thirteen decades in time, Nat. Phys. **12**, 171 (2016).

[55] H. Yang, G. Luo, P. Karnchanaphanurach, T.-M. Louie, I. Rech, S. Cova, L. Xun, and X. S. Xie, Protein conformational dynamics probed by single-molecule electron transfer, Science **302**, 262 (2003).

[56] D. Marinucci and P. Robinson, Alternative forms of fractional Brownian motion, J. Stat. Plan. Infer. **80**, 111 (1999).

[57] S. Sadegh, E. Barkai, and D. Krapf, 1/f noise for intermittent quantum dots exhibits non-stationarity and critical exponents, New J. Phys. **16**, 113054 (2014).

[58] A. A. Kurilovich, V. N. Mantsevich, K. J. Stevenson, A. V. Chechkin, and V. V. Palyulin, Complex diffusion-based kinetics of photoluminescence in semiconductor nanoplatelets, Phys. Chem. Chem. Phys. **22**, 24686 (2020).

[59] A. A. Kurilovich, V. N. Mantsevich, Y. Mardoukhi, K. J. Stevenson, A. V. Chechkin, and V. V. Palyulin, Non-Markovian diffusion of excitons in layered perovskites and transition metal dichalcogenides, Phys. Chem. Chem. Phys. **24**, 13941 (2022).

[60] G. Arfken and H. Weber, *Mathematical Methods for Physicists*, Mathematical Methods for Physicists (Harcourt/Academic Press, San Diego, California, 2001).